

Electric-field-tuned metallic fraction and dynamic percolation in a charge-ordered manganiteN. K. Pandey,¹ R. P. S. M. Lobo,² and R. C. Budhani¹¹*Department of Physics, Indian Institute of Technology Kanpur, Kanpur 208016, India*²*Laboratoire de Physique du Solide, Ecole Supérieure de Physique et Chimie Industrielles de la Ville de Paris, CNRS UPR 5, 75231 Paris Cedex 5, France*

(Received 24 October 2002; published 13 February 2003)

A percolative insulator-metal transition triggered by strong electric field is observed in epitaxial thin films of $(\text{Pr}_{0.65}\text{La}_{0.35})_{0.7}\text{Ca}_{0.3}\text{MnO}_3$. The field-driven metallic state is achieved in a regime of temperatures where the material is weakly ferromagnetic. Our experiments suggest that the metallic fraction reaches percolation threshold p_c at a field-dependent temperature T_{p_c} . A strong frequency dependence of complex ac resistance in the vicinity of T_{p_c} is consistent with the picture of percolative transport in a phase-separated medium.

DOI: 10.1103/PhysRevB.67.054413

PACS number(s): 75.30.Kz, 71.30.+h, 71.27.+a, 71.28.+d

The nucleation of charge delocalized ferromagnetic (CDFM) clusters in the charge ordered (CO) matrix of some narrow bandwidth manganites has attracted considerable attention in recent years.¹⁻⁶ The growth of this CDFM phase under strong external perturbations such as magnetic field, electric field, and photon and electron flux leads to a phenomenal drop in the resistivity of the material. This change in the resistivity is in fact much larger than the colossal magnetoresistance effect seen in a canonical, wide bandwidth ferromagnet such as $\text{La}_{2/3}\text{Sr}_{1/3}\text{MnO}_3$. The most exciting example of such CO manganites is the compound $\text{Pr}_{1-x}\text{Ca}_x\text{MnO}_3$ ($0.3 < x < 0.5$) and its derivatives in which the Pr and Ca sites are replaced by ions of larger size. In systems such as $\text{Pr}_{0.7}(\text{Ca}_{1-x}\text{Sr}_x)_{0.3}\text{MnO}_3$ (Refs. 7, 8) and $(\text{Pr}_{1-x}\text{La}_x)_{0.7}\text{Ca}_{0.3}\text{MnO}_3$ (Refs. 1,9) for example, the electron transport at $T < T_{\text{CO}}$ shows an insulator-metal transition with increasing strength of the magnetic field. Structural probes such as x-ray and neutron scattering, nuclear magnetic resonance, and transmission electron microscopy attest to the presence of the CDFM phase in these less than half filled CO manganites. High resolution electron microscopy studies of Cheong *et al.*¹ on $\text{La}_{5/8-y}\text{Pr}_y\text{Ca}_{3/8}\text{MnO}_3$ crystals show several thousand Å wide clusters dispersed in a commensurate (half filled) CO state, which presumably has charged defects. The mechanism of formation of the CDFM domains in these systems has been argued to be a disorder driven phase separation into equal electron density ferromagnetic and antiferromagnetic domains.¹⁰ Mayr *et al.*¹¹ have modeled the metal-insulator transition at $T < T_{\text{CO}}$ in the framework of a network of random resistors. The system is assumed to be percolative with metallic filaments whose number density increases with the magnetic field, in parallel with resistors of the insulating phase.

Electron transport in inhomogeneous materials with two or more phases of widely differing conductivity and size distribution is a complicated problem to analyze. Depending on the topology of the phases, electron transport has elements of tunneling, size quantization, and classical percolation with attendant nonlinearities.¹² Measurements of electric field and frequency dependent conductivity provide powerful means to identify the dominant transport process active in an inhomogeneous material.¹²⁻¹⁵

In this paper we investigate the phase separation driven insulator-metal transition in epitaxial films of the narrow

bandwidth manganite $(\text{Pr}_{0.65}\text{La}_{0.35})_{0.7}\text{Ca}_{0.3}\text{MnO}_3$ as a function of the amplitude and frequency of an ac field. While these samples show ferromagnetic (FM) ordering at $T_c \sim 120$ K, their low field dc response remains thermally activated above and below the FM ordering temperature. A strong electric field leads to growth of metallic channels, which are presumably ferromagnetic, at the expense of the charge ordered matrix and also through coalescence of the preexisting FM clusters. Our experiments also suggest that the metallic phase grows with temperature, and at a critical temperature (T_{p_c}) reaches the percolation threshold p_c . The T_{p_c} decreases as the electric field strength is raised. The ac resistivity at $T < T_c$ shows a strong frequency dependence typical of a percolating system where intercluster polarization and diffusion effects dominate the transport.^{14,15} This study provides an interesting case of dynamic percolation where the critical fraction p_c is a function of temperature.

Epitaxial thin films of the perovskite $(\text{Pr}_{1-x}\text{La}_x)_{0.7}\text{Ca}_{0.3}\text{MnO}_3$ were synthesized on (001) SrTiO_3 (STO) substrates using an excimer laser based (KrF, $\lambda = 248$ nm) pulsed laser deposition (PLD) system. The substrate temperature, oxygen partial pressure, and pulse energy density during ablation were 800 °C, 400 mTorr and 3 J/cm², respectively. The surface quality of the STO substrates supplied by a commercial vendor of epitaxial quality substrates was further improved through a buffered HF treatment.¹⁶ Details of film deposition and characterization of various manganites are given elsewhere.^{17,18} We have used standard θ - 2θ x-ray diffraction and electron probe microanalysis to ascertain the structure and chemical composition of the films, respectively. Measurements of resistivity and current voltage (I - V) characteristics were performed on ~ 4500 Å thick films employing both dc and ac techniques. In the first case, a fixed or variable voltage was impressed on the sample and the current flow was monitored by measuring the voltage drop across a metal film resistor. For measurements of conductivity as a function of frequency we used a two-phase digital lockin amplifier and a function generator. The temperature and field dependent magnetization of the samples was measured in a MPMS 5 T Quantum Design superconducting quantum interference device magnetometer.

Charge ordering in the compound $\text{Pr}_{0.7}\text{Ca}_{0.3}\text{MnO}_3$ manifests itself as a step in the resistivity at $T \sim 210$ K.⁸ Below

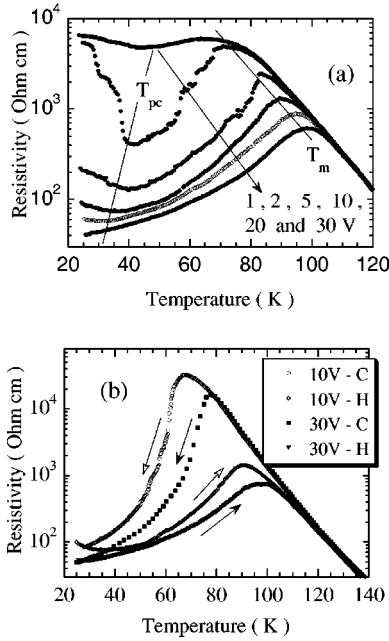


FIG. 1. Panel (a) shows resistivity of the sample measured in a constant electric field mode. A potential of 1 V corresponds to 66 V/cm electric field. The characteristic temperatures T_m and T_{pc} are explained in the text. The behavior of resistivity during cooling and heating cycles is shown in panel (b).

this temperature (T_{CO}), the resistivity is thermally activated. The resistivity of these samples at the lowest temperature drops as more and more Pr sites are replaced by the larger La^{3+} ions.^{1,9,19} At $La/Pr \sim 1$, the e_g bandwidth becomes sufficiently large such that a typical CDFM behavior is seen in the resistivity. This tendency for a transition from CO to CDFM state with increasing x makes the CO state in sample with $x=0.35$ the most precarious, and prone to melting under external perturbations. In this paper we focus on the percolative nature of transport as the CO state breaks down on application of strong electric field. In Fig. 1(a) we show the resistivity of the sample with $x=0.35$ measured as a function of increasing temperature in a constant electric field mode. At low fields (<66 V/cm), the resistivity remains insulating in the temperature window of 80 to 300 K. However, below ~ 80 K the thermally activated conduction is truncated by a competing process which is related with the onset of ferromagnetic order as discussed in the following sections. The saturation value of the resistivity is higher by a factor of ~ 10 compared to the data on single crystals of $Pr_{5/8-y}La_yCa_{3/8}MnO_3$ (Ref. 1) with the same Pr/La ratio as in our films. There are two possible reasons for this difference: (i) a lower Ca concentration in the films compared to the crystals and (ii) structural defects introduced as a result of stress relaxation in these relatively thick (~ 4500 Å) film grown on STO where the lattice mismatch is $\sim 2\%$. On increasing the field to ~ 130 V/cm, the resistivity first drops with temperature and then shows a metal like behavior (positive dp/dT) over the window defined by the temperatures T_{pc} and T_m . The lowest temperature (≈ 20 K) resistivity of the sample drops and the metallic regime widens as the

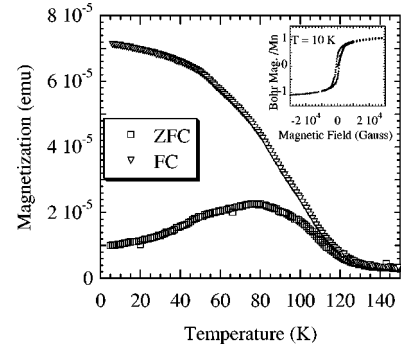


FIG. 2. Field-cooled (FC) and zero-field-cooled (ZFC) magnetization of a $(Pr_{0.65}La_{0.35})_{0.7}Ca_{0.3}MnO_3$ film measured in a 100 G. Inset shows variation of the magnetic moment with field at 10 K.

strength of the electric field is increased. However, beyond the field dependent temperature T_m , the resistivity becomes independent of the field. The high field and low field data nicely collapse between T_m and ~ 120 K. At still higher temperatures, however, effects of sample heating in measurements performed at larger values of electric field result in separation of the curves. We have limited high field measurements to ~ 130 K in order to avoid sample heating. The characteristic temperature T_m shows supercooling and superheating effects as evident in Fig. 1(b). The T_m is lower in a cooling measurement and the cooling and heating curves encompass a large hysteresis. In Fig. 2 we show the zero-field-cooled (ZFC) and field-cooled (FC) magnetization of this sample measured at 100 G. The onset of ferromagnetic ordering is seen at $T \sim 120$ K. A large splitting between the FC and ZFC branches of magnetization suggest presence of large ferromagnetic clusters whose moments freeze below a certain temperature. This observation is consistent with the earlier reports on similar narrow bandwidth manganites where clusters of the FM phase nucleate at $T < T_{CO}$. The inset of Fig. 2 shows the magnetic field dependence of magnetization at 10 K. While a ferromagnetic coupling of all Mn^{3+} and Mn^{4+} spins should lead to an average site spin of $\sim 3.8\mu_B$, the saturation magnetization is only $\sim 1\mu_B$ in this case. This suggests that a significant fraction of the material remains in the antiferromagnetic CO state. Since the FM phase is metallic due to double exchange,²⁰ whereas the CO phase is insulating, the transport in this inhomogeneous system will have elements of spin-dependent tunneling and percolation. A plausible scenario for transport, which qualitatively explains the data of Figs. 1 and 2 is as follows: At $T < T_m$, we assume a random distribution of well separated CDFM clusters with uncorrelated bulk magnetization at the lowest temperature. At low electric fields, the transport through such a matrix is controlled by the CO phase and the resistivity remains insulating throughout the temperature range. Based on the published magnetization²¹ and optical reflectivity²² data, we argue that the relative fraction of the CDFM clusters increases with the electric field. While a microscopic mechanism of this is not known, one plausible explanation is based on electric field induced breakdown of the thinnest insulating regions separating the CDFM clusters. In the intermediate field regime, the fraction of the CDFM

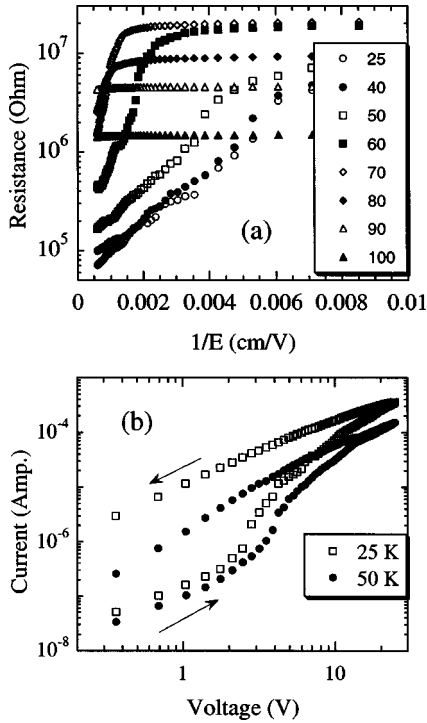


FIG. 3. Panel (a) shows resistance of the sample at several temperatures plotted as a function of the inverse of applied electric field. For measurements at each temperature, the sample was cooled from ~ 200 K. The forward and reverse branches of I - V curves at 25 and 50 K are shown in panel (b). Arrows mark the direction of voltage sweep.

phase at temperatures below the minimum in the resistivity ($T < T_{p_c}$) is still not enough to provide a conducting channel across the sample. But as the temperature grows, magnetic moment on the clusters become relatively free to rotate and the spin barrier for tunneling disappears with an increasing rate. This facilitates nearest neighbor tunneling. A situation eventually develops in which the local electric field between two parallel spin clusters becomes so large that a nonconducting link separating them breaks down. In this model of transport, the critical fraction p_c at which an infinite conducting backbone develops is a function of temperature. The minimum in the resistivity corresponds to this temperature (T_{p_c}). The resistivity of the sample at $T > T_{p_c}$ is metallic. This dynamic percolation threshold temperature is shifted to lower values at the higher and higher electric fields. At the highest field, an infinite conducting backbone exists even at the lowest temperature. These conducting channels will eventually close when the temperature exceeds the Curie temperature. However, at the higher temperatures, the resistivity of the CO matrix is low enough to yield a smooth transition from metallic to insulating behavior as T exceeds T_m .

We now substantiate this picture of a dynamic percolating system through measurements of current-voltage (I - V) characteristics and complex ac resistance. Figure 3(a) shows the dc resistance vs $1/E$ plots at several temperatures. Two characteristic features of these data are noteworthy. (i) The resistivity at low temperatures is nonlinear over most of the field (E) range, but for a small linear region at the lowest field. (ii)

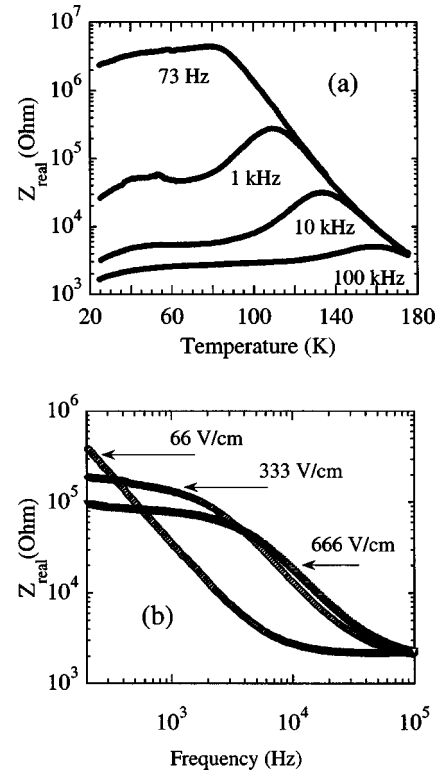


FIG. 4. Panel (a) shows the real part of complex impedance as a function of temperature. The data shown are at several frequencies of the ac driving voltage (1 V peak-to-peak). Panel (b) shows frequency dependence of impedance at 30 K for three excitation voltages.

The critical value of the field at which nonlinearity sets in increases with temperature. At high temperatures, the data are linear over the entire field range. At a first glance, the broad features of the data shown in Fig. 3(a) are similar to the behavior of electric field dependent resistivity in granular metal films.¹² Here the nonlinearity comes from electric field induced tunneling between isolated metal particles. The resistance varies as $R = R_0 \exp(E_0/E)$ at high fields and the behavior is linear below a critical field at which the thermal energy $k_B T$ becomes larger than $e \Delta V$, where ΔV is the voltage difference between the grains involved in tunneling. However, the temperature dependence of resistivity in the linear as well as nonlinear regimes remains thermally activated. While this picture may be applicable at low temperatures where $d\rho/dT$ is negative, it is certainly not consistent with the positive $d\rho/dT$ at $T > T_{p_c}$. Furthermore, the field-induced tunneling process is expected to be reversible. In Fig. 3(b) we show two typical I - V curves of the sample taken at 25 and 50 K. The large hysteresis seen in the data is indicative of an irreversible process. The field-reversed branch of the I - V curves is Ohmic. Moreover, this field-driven Ohmic behavior persists when the measurement is repeated at the same temperature. Our I - V measurements show that a metallic channel once opened by strong field remains open unless the pristine state of the sample is recovered by heating it above the charge ordering temperature.

The broad features of the data shown in Figs. 1–3 can

now be understood on the basis of a phenomenological model for percolative metal-insulator transition. This is based on the concept of a dynamic random resistor network (DRRN).^{23,24} The microscopic mechanism responsible for the dynamic resistance may be tunneling across a thin CO layer followed by breakdown of the CO state and opening up of a permanent metallic link. The I - V characteristics of a DRRN system are expected to take the form $V=R_0I+R_1I^\alpha$, where $\alpha>1$. The nonlinearity sets in above a threshold current. Furthermore, the I - V curves of a DRRN show avalanche effects and irreversibility. These features are evident in the data of Fig. 3(b).

A further confirmation of the electric field induced growth of metallic clusters and ensuing percolative transport comes from the measurements of ac resistance. In Fig. 4(a) we show the resistance (inverse of the real part of ac conductance) of the sample as its temperature is raised from 20 K. These measurements have been performed at different frequencies while the electric field strength was held constant at ~ 66 V/cm (peak-to-peak). As seen in panel (a) of Fig. 4, the resistance at lower temperatures drops with the increase in frequency. However, this dependence is truncated above a frequency dependent temperature $T_m(\omega)$ at which R goes through a maximum. We note an interesting identity between the T_m of Fig. 1, which increases with E_{dc} and the $T_m(\omega)$ which increase with the frequency. Figure 4(b) shows R vs ω curves at 30 K taken at the electric field strength of 66, 330, and 660 V/cm. The shape of these curves changes dramatically as we increase the field strength. At the lowest field, the resistance decreases with frequency as $R\sim\omega^{0.86}$. This behavior is characteristic of transport in a system where the metal-

lic fraction is below the percolation threshold.^{25,26} A strikingly different ω dependence is seen at the higher electric fields. Here, the resistance first remains frequency independent and then there is a sharp drop when $\omega\geq 10$ kHz. This anomalous frequency dependence is typical of a percolating system near p_c .^{25,26} Two different effects, intercluster polarization¹⁴ and anomalous diffusion¹⁵ have been considered to explain the anomalous response. The former emphasizes capacitive coupling between metallic clusters, which become large near p_c due to the reduced barrier thickness between finite size clusters. The alternative explanation takes into account the delay time introduced by diffusion through the tenuous structure of the infinite conducting cluster as $p\rightarrow p_c$ from the metallic side.

In summary, we observe an electric field induced insulator-metal transition in epitaxial films of $(\text{Pr}_{0.65}\text{La}_{0.35})_{0.7}\text{Ca}_{0.3}\text{MnO}_3$. The transition occurs in the temperature regime where a ferromagnetic phase, presumably in cluster form, coexists with the charge ordered phase of this manganite. Measurements of complex ac resistance with excitation of variable frequency and amplitude, dc current-voltage characteristics and irreversibility in heating and cooling cycles, indicate a percolative I - M transition. This system presents an interesting case of dynamic percolation characterized by a temperature and electric field dependent percolation threshold.

This research has been supported by a grant from the Science and Engineering Research Council of the Department of Science and Technology, Govt. of India. We thank Professor R. Prasad and Dr. P. Monod for helpful discussions.

-
- ¹M. Uehara, S. Mori, C. H. Chen, and S. W. Cheong, *Nature* (London) **399**, 560 (1999).
- ²C. N. R. Rao and A. K. Raychaudhuri, in *Colossal Magnetoresistance, Charge Ordering and Related Properties of Manganese Oxides*, edited by C. N. R. Rao and B. Raveau (World Scientific, Singapore, 1998), p. 1.
- ³Y. Tokura and Y. Tomioka, *J. Magn. Magn. Mater.* **200**, 1 (1999).
- ⁴E. Dagotto, T. Hotta, and A. Moreo, *Phys. Rep.* **344**, 1 (2001).
- ⁵W. Prellier, Ph Lecoq, and B. Mercey, *J. Phys.: Condens. Matter* **13**, R915 (2001).
- ⁶M. Saloman and M. Jaime, *Rev. Mod. Phys.* **73**, 583 (2001).
- ⁷B. Raveau, A. Maignan, and V. Caignaert, *Solid State Commun.* **117**, 424 (1995).
- ⁸H. Yoshizawa, R. Kajimoto, H. Kawano, Y. Tomioka, and Y. Tokura, *Phys. Rev. B* **55**, 2729 (1997).
- ⁹N. A. Babushkina, L. M. Belova, D. I. Khomskii, K. I. Kugel, O. Yu. Gorbunov, and A. R. Kaul, *Phys. Rev. B* **59**, 6994 (1999).
- ¹⁰Adriana Mario, Matthias Mayr, Adrian Feiguin, Seiji Yonuki, and Elbio Dagotto, *Phys. Rev. Lett.* **84**, 5568 (2000).
- ¹¹Matthias Mayr, Adriana Mario, Jose Verges, Jeanette Arispe, Adrian Feiguin, and Elbio Dagotto, *Phys. Rev. Lett.* **86**, 135 (2000).
- ¹²B. Abeles, Ping Sheng, M. D. Coutts, and Y. Arie, *Adv. Phys.* **24**, 407 (1975).
- ¹³J. P. Clerc, G. Giraud, J. M. Laugier, and J. M. Luck, *Adv. Phys.* **39**, 191 (1990).
- ¹⁴David Bergman and Yoseph Emery, *Phys. Rev. Lett.* **39**, 1222 (1977).
- ¹⁵Yoav Gefen, Amnon Ahrony, and Shlomo Alexander, *Phys. Rev. Lett.* **50**, 77 (1983).
- ¹⁶M. Kawasaki, K. Takahashi, T. Maeda, R. Tsuchiya, M. Shinohara, O. Ishiyama, T. Yonezawa, M. Yoshimoto, and H. Koinuma, *Science* **266**, 1540 (1994).
- ¹⁷P. Padhan, N. K. Pandey, S. Srivastava, R. K. Rakshit, V. N. Kulkarni, and R. C. Budhani, *Solid State Commun.* **117**, 27 (2001).
- ¹⁸S. Srivastava, N. K. Pandey, P. Padhan, and R. C. Budhani, *Phys. Rev. B* **62**, 13 868 (2000).
- ¹⁹D. E. Cox, P. G. Radaelli, M. Marezio, and S.-W. Cheong, *Phys. Rev. B* **57**, 3305 (1998).
- ²⁰C. Zener, *Phys. Rev.* **82**, 403 (1951).
- ²¹Ayan Guha, N. Khare, A. K. Raychaudhuri, and C. N. R. Rao, *Phys. Rev. B* **62**, R11 941 (2000).
- ²²M. Feibig, K. Mayano, Y. Tomioka, and Y. Tokura, *Science* **280**, 1925 (1998).
- ²³Yoav Gefen, Wie-Heng Shih, Robert B. Laibowitz, and J. M. Viggiano, *Phys. Rev. Lett.* **57**, 3097 (1986).
- ²⁴D. R. Bowman and D. Stroud, *Phys. Rev. B* **40**, 4641 (1989).
- ²⁵R. B. Laibowitz and Yuval Gefen, *Phys. Rev. Lett.* **53**, 380 (1984).
- ²⁶Yi Song, T. W. Noh, Sung-Ik Lee, and James R. Gaines, *Phys. Rev. B* **33**, 904 (1986).